Autonomous track before detection of a radio target by an unmanned aerial vehicle using radio signal strength measurement

A. Firouzabadi[1], S. M. Esmailifar[1*], and A. Jafargholi [2]

[1] Department of Aerospace Engineering, Amirkabir University of Technology, Tehran, Iran
[2] Electromagnetic and Antenna lab, Department of Physics, Amirkabir University of Technology, Tehran, Iran

ABSTRACT: This paper presents a Track-Before-Detect (TBD) approach to search and localize a radio-emitted target in a wide marine environment using just the received signal strength (RSS) measurements. In this problem, the lost target transmits radio signals, and the unmanned aerial vehicle (UAV), guided on a search path, receives the target transmitted signal strength by its mounted antenna. The guidance law directs the UAV to the best detection points where the probability of target detection is maximum. At the same time, the estimation module evolves the posterior distribution of the radio target states, including the target position, heading, and transmitter power. The best detection points are calculated based on this evolved target's states' posterior. The superiority of the proposed method is due to the consideration of the antenna radiation pattern, which is accurately modeled in this paper and ensures the strength of the filter against the uncertainties of the measurement model and the target model. The simulation results validate the performance of the proposed method in the autonomous localization of a lost moving target.

1- Introduction

In recent years, the prominent empowerment of unmanned aerial vehicles made them an efficient platform for realizing complicated military and civil missions. Autonomous search, detection, and tracking of a ground target is still a challenging mission in which UAVs can play an important role. In this regard, The UAV task is extracting target states from all information measured by the UAV's onboard sensors. Depending on the capabilities of the sensor, this information can be visual [1], thermal [2], radio [3], or acoustic [4]wherein the sources are simultaneously emitting identical acoustic signals. Distributed coordinated localization algorithms based on multiple range and direction measurements are presented and performances are evaluated in different practically significant mission scenarios. Non-deterministic polynomial (NP. There are several applications, such as traffic monitoring [5], environmental monitoring [6], wildlife tracking [7], [8], border patrol, and combat scenarios [9], which can be classified as target search and localization. Marine applications such as a damaged ship or lost lifeboats search and rescue, enemy threat recognition and ward off, or even stop illegal sea-border crossings are missions in which target detection and localization time play a vital role in life-saving, especially in adverse sea and weather conditions.

Localization of radio frequency (RF) sources can be implemented by different measured characteristics of the radio signal, so-called metrics, such as time-of-arrival (ToA) [10], time-difference-of-arrival (TDoA) [11], roundtrip time (RTT) [12], angle-of-arrival (AoA) [13] and received signal strength (RSS) [14], [15]. RSS-based methods are more popular among these, mainly due to low complexity and hardware requirements.

There are many localization techniques to extract the target states based on noisy RSS metrics by static or dynamic approaches. Trilateration [16], least square methods [17], and maximum likelihood (ML) [18] are some static methodologies that do not take into account the target dynamics and observation history. This leads to limitations on localizing and tracking a moving target, especially in the presence of un-modeled multipath interference. [19] investigated five linear least square (LLS) based localization algorithms for RF signal source search and localization (SSSL) as the UAV navigates autonomously along a path with predefined waypoints. They assumed a simplified propagation channel model for The UAV network that does not include the realistic antenna characteristics and propagation conditions.

Dynamic approaches aim to locate the target by integrating all information from incoming periodic observations and predictions of the target movement, which makes them more effective in similar scenarios. RSS-based linear estimator

*Corresponding author's email: abdefy@aut.ac.ir

like Extended Kalman Filter (EKF) is utilized for target localization [20]. In [21], the Hidden Markov Model (HMM) and EKF are combined to mitigate line-of-sight blockage errors. In [22], EKF is used to update the estimation of an aerial target location. They also have developed a predictive path planning strategy based on the Fisher information matrix (FIM) to find the trajectory that maximizes the received information. In [3], a grid-based filter is presented to localize radio-tagged wildlife using a small UAV. They assumed that the radio tag was observable from the beginning of the search, which is not a realistic assumption. In [23], a gradient-based waypoint optimization for two UAVs equipped with TOA sensors has been developed for the passive localization of a stationary radio source with omnidirectional propagation. The control strategy is based on the position error covariance estimated by the EKF.24]] proposed an unscented Kalman filter (UKF) algorithm combined with radio frequency identification (RFID) for target positioning and tracking by a UAV equipped with an RFID reader based on received signal strength indication (RSSI) measurements.

Traditional radar tracking algorithms correlate a set of point measurements recorded by sensors in each scan over time and estimate positional/kinematic characteristics (such as Doppler-azimuth range). A poor signal-to-noise ratio (SNR) of the measured signal reduces the target detection performance. A common approach for tracking in low SNR environments is to set the detection threshold very low and let the tracking algorithm deal with the high rate of clutter and false alarm detection. In this paper, it is assumed that there is no information about the target's dynamics and location, and the tracking is performed using only low-cost passive RSSI sensors. Therefore, the difficulty of the estimation is due to the sensors' inabilities and low SNR measurements that cause not detecting the target with a few measurements. A potentially more powerful approach, referred to as Track-Before-Detect (TBD), tracks the possible presence of the targets (target's posterior) until the detection occurs. The TBD approach improves tracking performance and allows the tracking filter to effectively deal with poorly observed targets, i.e. targets with low SNR.

The main difficulty in the TBD approach is that the measurement, a highly nonlinear function of the target state. Dynamic Localization by using particle filters is capable of dealing with nonlinear dynamics and measurement models and non-Gaussian noises [25]. This filter has been used by a number of authors for the TBD approach. In [26], a particle filter solution is proposed for localizing a known radio source using only RSS. They assumed an ideal empirical radio model for signal propagation. In [27], the localization of VHF radio-tagged animals by a UAV is demonstrated. They utilized a particle filter for localizing and a partially observable Markov decision process (POMDP) for dynamic path planning. This approach guides the UAV toward maximum information gain to detect multiple mobile animals and reduce detection time. A cooperative localization algorithm of marine targets by multiple UAVs has been developed in [28], [29]. A modified

Monte-Carlo filter, considered a Track-Before-Detect (TBD) filter, has been used to estimate the posterior of the target by fusing the UAVs' observations. They also presented a heuristic searching guidance law to direct the UAVs to the guidance points where the best observations are available for an optimum search.

Saghafi and Esmailifar [30] employed a UAV equipped with an RSS-based omnidirectional antenna for searching and localizing a lost target utilizing Bootstrap filtering and searching guidance law together with a BTT acceleration autopilot. They assumed that the transmitter and receiver antenna gain patterns are spherical, which is not an accurate assumption. Here, we develop a TBD approach for target search and localization, capable of handling realistic antenna patterns. In this regard, receiver and transmitter antennas are designed, and their signal radiation patterns are modeled accurately. So, the contributions of this work are itemized as follows:

- Development of a TBD approach to localize an unknown radio target in the presence of noises and uncertainties, especially in a low SNR environment.
- Both the transmitter and receiver antennas are designed and customized with an accurate radiation pattern model for a search and rescue scenario in a large-scale environment. This design provides an accurate measurement model for application in the TBD approach as well as for more accurate evaluation of the tracking algorithm using approximate radiation patterns in software-in-the-loop (SIL) simulation.
- Applying a search approach utilizes a heuristic searching guidance law and guidance points.

These modifications make the measurement model of the search and localization filter more accurate and increase the target states' observability, leading to faster localization. The search approach applies more appropriate maneuvers to the UAV to capture more efficient signals and also guides it to the best detection point where the measured signal maximizes the probability of detection, resulting in less localization error in low SNR environments.

In this regard, the paper is organized as follows: After the introduction (section 1), the search and localization algorithm is described based on the Bayesian estimation procedure and its implementation by sequential Monte Carlo (SMC) in section 2. Since one of this paper's contributions is the utilization of a more accurate RSS measurement model in the Bayesian filter, in section 3, the antenna simulation of its far-field propagation model will be explained. After the development of the target search and localization algorithm in previous sections, it is the turn of the UAV dynamic and guidance simulation for statistical evaluation of the developed algorithm. Therefore, in section 4, the guidance law for directing the UAV on the search path is introduced, and the translational and rotational dynamics of the UAV are explained in section 5. Simulation results are provided in section 6, and finally, a conclusion is made in section 7.
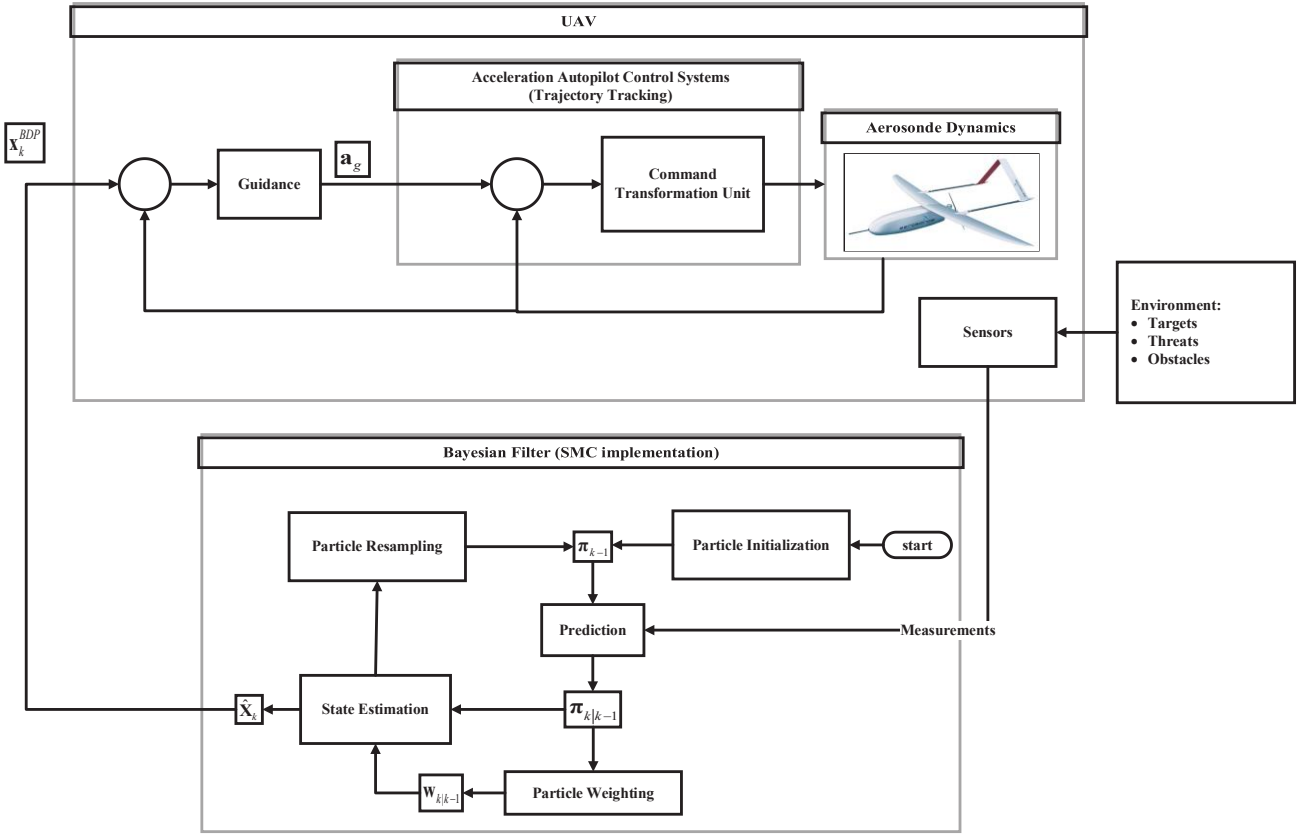
Fig. 1. Framework of the cooperative multi-target tracking.

2- Target localization

Localizing in a broad environment where the prior probability distribution of the target is indistinct and non-Gaussian complicates the estimation problem. Contrary to the Kalman filter, the SMC filter can handle this complicated condition with much more computational effort [31].

The framework of the radio target tracking problem is illustrated in Fig. 1, which it shows the contribution between estimation, guidance, and control modules. In the following, each module will be explained in detail.

2- 1- Target state estimation

As previously mentioned, the search and localization scenario is defined as follows:

The lost target, which might be a damaged ship, lost lifeboat, threatening battleship, or other marine vehicles, located within a marine environment, is denoted by "t". This target transmits a radio signal received and measured by a UAV's onboard sensor denoted by "s". Since there is no information about target motion, its dynamics are modeled as a random walk motion:

$$\mathbf{x}_k^t = \mathbf{f}_{k-1}(\mathbf{x}_{k-1}^t, \mathbf{w}_k) = \mathbf{x}_{k-1}^t + \mathbf{w}_k, \tag{1}$$

where $\mathbf{x}_k^t$ is the state vector of the target and $\mathbf{w}_k$ is the dynamic noise vector due to the unknown target behavior; both are considered at the time step k. The target state vector has four components: target location $\begin{bmatrix} x_k^t & y_k^t \end{bmatrix}^T$, target heading ψ_k^t, and transmitter antenna power P_t. The UAV onboard sensors can measure the received signal strength, which is the function of the UAV location, $\mathbf{x}_k^s$, the target location, $\mathbf{x}_k^t$, and measurement noise, $\mathbf{v}_k$, as:

$$\mathbf{x}_k^t = \mathbf{f}_{k-1}(\mathbf{x}_{k-1}^t, \mathbf{w}_k) = \mathbf{x}_{k-1}^t + \mathbf{w}_k, \tag{2}$$

In the above equation, the navigation system obtains the UAV location, and the target location will be estimated from the sensor's measurements by the SMC filter. The measurement model is presented in section 3.

The Bayesian approach estimates the system states ($\mathbf{x}_k^t$) by constructing the posterior probability density function (pdf or density) of the states based on all available information, including the sequence of received measurements ($\mathbf{z}_{1:k}$). On the other hand, estimation proceeds by calculating marginal posterior distribution $p(\mathbf{x}_k^t \mid \mathbf{z}_{1:k})$ sequentially through prediction (3) and update (4) steps:

$$p(\mathbf{x}_k^t \mid \mathbf{z}_{1:k-1}) = \int p(\mathbf{x}_k^t \mid \mathbf{x}_{k-1}^t) p(\mathbf{x}_{k-1}^t \mid \mathbf{z}_{1:k-1}) d\mathbf{x}_{k-1}^t, \tag{3}$$

where, $p(\mathbf{x}_k^t \mid \mathbf{x}_{k-1}^t)$, is determined based on the probabilistic Markov model of the target (1). Also, $p(\mathbf{x}_{k-1}^t \mid \mathbf{z}_{1:k-1})$ is the prior distribution calculated in the update stage of the last time step k-1. The update step is as follows:

$$p(\mathbf{x}_k^t \mid \mathbf{z}_{1:k}) = \frac{p(\mathbf{z}_k \mid \mathbf{x}_k^t) p(\mathbf{x}_k^t \mid \mathbf{z}_{1:k-1})}{\int p(\mathbf{z}_k \mid \mathbf{x}_k^t) p(\mathbf{x}_k^t \mid \mathbf{z}_{1:k-1}) d\mathbf{x}_k^t}, \tag{4}$$

where $p(\mathbf{z}_k \mid \mathbf{x}_k^t)$, the likelihood function is determined by the measurement model (2).

2- 2- SMC implementation of the Bayesian filter

In the case of a nonlinear system or non-Gaussian noises and prior, there is no general closed-form solution for the Bayesian recursion and $p(\mathbf{x}_k^t \mid \mathbf{z}_{1:k})$. Therefore, the SMC filter, introduced by Gordon [32], will be implemented as an approximate solution for Bayesian filtering. The SMC filter represents the posterior distribution by N samples and their corresponding weights:

$$p(\mathbf{x}_k^t \mid \mathbf{z}_{1:k}) \approx \sum_{i=1}^{N} w_k^i \delta(\mathbf{x}_k^t - \mathbf{x}_k^i), \tag{5}$$

where $\delta(x)$ is the Dirac delta function.

It is impossible to Draw a set of random samples from any distributions such as $p(\mathbf{x}_k^t \mid \mathbf{z}_{1:k})$ except for some well-known ones (uniform, normal and beta etc. distributions); then, in an alternate approach, an importance density function $q(\mathbf{x}_k^i \mid \mathbf{x}_{k-1}^i, \mathbf{z}_k)$ is introduced, which can generate new samples based on Monte-Carlo integration by knowing the last time step samples and their corresponding weights [33]. The weights are updated in such a way to compensate using importance density instead of posterior:

$$w_k^i = w_{k-1}^i \frac{p(\mathbf{z}_k \mid \mathbf{x}_k^i) p(\mathbf{x}_k^i \mid \mathbf{x}_{k-1}^i)}{q(\mathbf{x}_k^i \mid \mathbf{x}_{k-1}^i, \mathbf{z}_k)}, \tag{6}$$

in which all the weights should be normalized such that $\sum_{i=1}^{N} w_k^i = 1$.

Drawing the samples from importance density and updating the corresponding weights are the steps of the sequential importance sampling (SIS) algorithm. In this method, the minimum mean-square error (MMSE) is converted to

$$\hat{x}_k^{MMSE} = \sum_{i=1}^{N} w_k^i \mathbf{x}_k^i \tag{7}$$

And the estimation covariance is

$$\mathbf{P}_k = \sum_{i=1}^{N} w_k^i \left(\mathbf{x}_k^i - \hat{x}_k^{MMSE} \right) \left(\mathbf{x}_k^i - \hat{x}_k^{MMSE} \right)^T \tag{8}$$

In the SIS algorithm, degeneracy, which means that the variance of importance weights increases over time, is inevitable. The degeneracy of samples can be measured by

$$N_{eff} = \frac{1}{\sum_{i=1}^{N} (w_k^i)^2} \tag{9}$$

where N_{eff} is inversely related to the degeneracy problem. Therefore, the degeneracy shows up when N_{eff} becomes less than a threshold value N_T. In the present research, the resampling technique is utilized to reduce the sample degeneracy in which the samples with small weights are replaced by those with larger weights. Resampling and other techniques, like the injection method, are discussed in [34] in detail.

3- Measurement model

In this section, the accurate model of radio signal propagation is used for the measurement model. Therefore, after introducing the Friis propagation model, appropriate transmitter and receiver antennas are designed, and then their far-field propagation patterns are modeled. It is worthwhile to mention that this model is used for

the measurement model required in the Bayesian filter process (Eq. (2)) and also for

the measurement model utilized for simulations.

These two models might not be the same because, in the real world, we have mismatched modeling between the filtering measurement model and real-world electromagnetic propagation. In the following sections, we discuss more about this modeling mismatch.

3- 1- Friis free space propagation model

The Friis propagation model describes the attenuation of radio energy between two antennas. In this model, it is assumed that the space between the transmitter and receiver antennas, R, is free of any object that can absorb or reflect the energy of the radio frequency waves. This model is as follows:

$$P_s = \left(G_t(\varphi^t, \theta^t) G_s(\varphi^s, \theta^s) \left(\frac{\lambda}{4\pi R} \right)^2 \right) P_t, \tag{10}$$

where P_s is the received power, P_t is the transmitted power, $G_s(\varphi^s, \theta^s)$ is the receiver antenna gain, $G_t(\varphi^t, \theta^t)$ is the transmitter antenna gain, and λ is the signal wavelength [35].
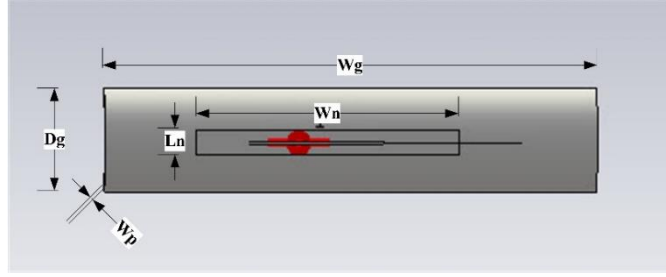
(a)
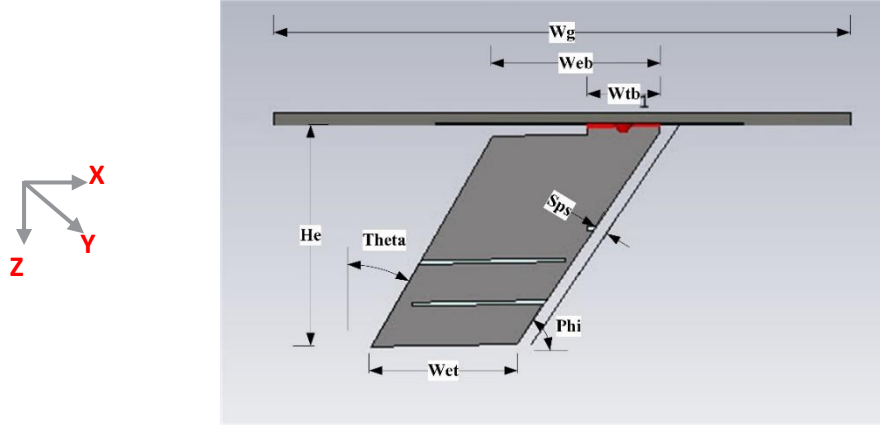
(b)

Fig. 2.The schematic of the blade antenna and its design parameters: (a) Top view, (b) Side view.
Wg = 60 mm, Wn=32 mm, Ln = 3 mm, Dg = 13 mm, Wp = 1 mm, Web = 17 mm, Wtb = 7 mm, Sps = 2 mm,
Wet = 15 mm, He = 22.65 mm, Phi = 55 degree, Theta = 30 degree.

Using the Friis equation, the measurement Eq. (2), would be expressed as:

$$z_k = \left(G_t(\varphi_k^t, \theta_k^t) G_s(\varphi_k^s, \theta_k^s) \left(\frac{\lambda}{4\pi \sqrt{(x_k^t - x_k^s)^2 + (y_k^t - y_k^s)^2 + (z_k^s)^2}} \right)^2 \right) P_{t_k} + v_k, (11)$$

where v_k is the measurement noise, which represents the fading or shadowing effects. In the case of fast fading, the Gaussian distribution does not properly model the noise, so v_k should be replaced by either a Rayleigh or Ricean distributions [36].

In the following sections, first, the transmitter and receiver antennas are designed, and then for obtaining the antennas' gains $G_t(\varphi^t, \theta^t)$ and $G_s(\varphi^s, \theta^s)$, their propagation patterns are modeled.

3- 2- Antenna design
Blade antennas are suitable for airborne applications due to their compact size, lightweight, and aerodynamic shape, resulting in minimal weight and drag penalties. Helical antennas can receive and transmit high gain, wide bandwidth, and circular polarization radiation, which are highly demanded for airborne tracking. Therefore, a blade

antenna is assumed to be mounted under the UAV to receive the radio signals transmitted by the marine lost target utilizing a helix antenna. To analyze the proposed antennas, the CST Microwave simulator is used. Both antennas are customized based on the 2.4 GHz frequency band, which is almost legal to operate without a license worldwide. The schematic of the blade antenna is depicted in Fig. 2 and the parameters are labeled in the figure captions.

The normalized simulated far-field radiation of the blade antenna is depicted in Fig. 3 at f = 2.4 GHz. It is clear that a dipole-like behavior is observed. The antenna had a cross-polarization discrimination of >20 dB, at the main lobe direction. The finite ground plane and the antenna's asymmetrical structure lead to having asymmetrical radiation pattern. It should be noted that due to the asymmetry of the radiator, it is expected to have an asymmetrical radiation pattern.

The schematic of the helix antenna is depicted in Fig. 4. The antenna design parameters are labeled in the figure caption. The normalized simulated far-field radiation of the helix antenna is depicted in Fig. 5. According to this figure, since, the position and orientation of UAV antenna will change during the search, the comparable co- and cross-polarization components are accordingly suitable.

(a)   (b)
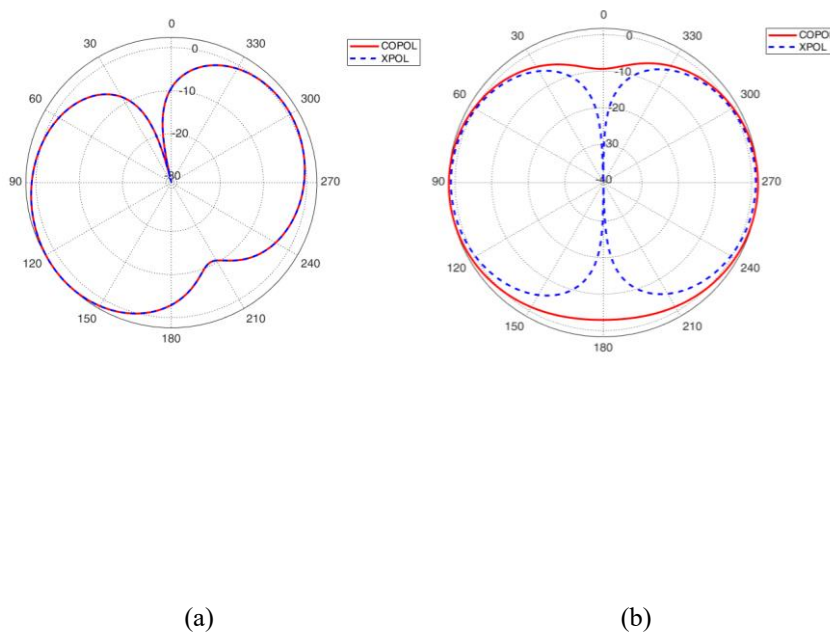
Fig. 3. The normalized radiation pattern of the blade antenna for (a) E-plane, (b) H-plane.
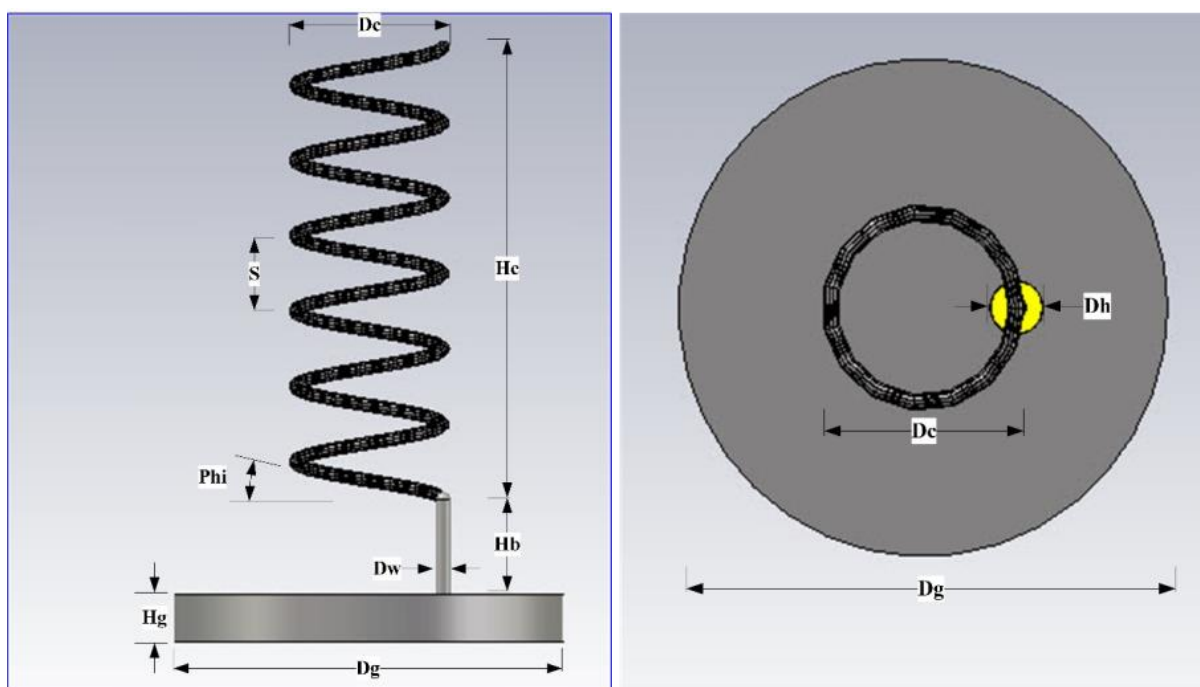
Fig. 4. The schematic of the helix antenna and its design parameters. (a) Side view, (b) Top view.
Dg = 25 cm, Dc = 10 cm, Dw = 1 cm, Dh = 3 cm, Hc = 29 cm, Hb = 7 cm, Hg = 3 cm, S = 5 cm,
Phi = 13 degree.
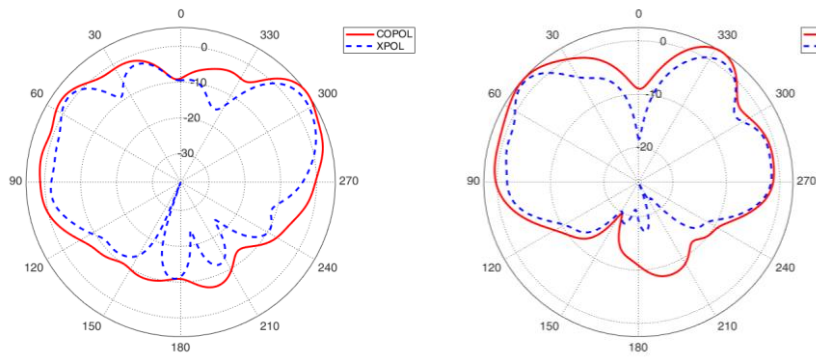
(a)   (b)

Fig. 5. The normalized radiation pattern of the blade antenna for: (a) E-plane, (b) H-plane.
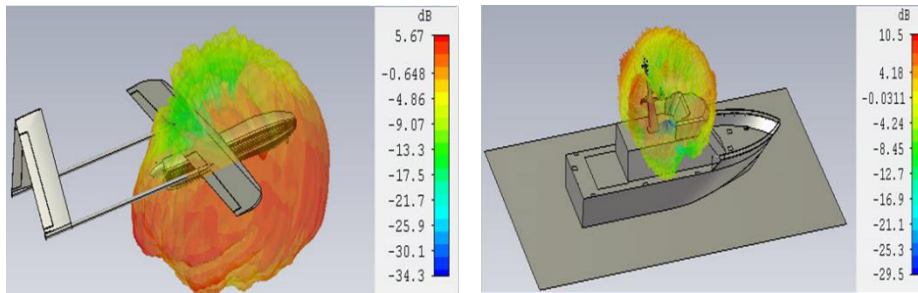
(a)   (b)

Fig. 6. Tridimensional far-field radiation pattern of the (a) blade, and (b) helix antennas.

3- 3- Mounted antennas on the UAV and the lost target

In order to have a more accurate model, in this part, the radiation patterns of the antennas are simulated when they are mounted on the UAV and the lost target (for example, a ship on the sea). Fig. 6 depicts the far-field radiation pattern of the blade and helix antennas that are installed under the UAV and on a ship, respectively. The gain of the receiver $G_s(\varphi^s,\theta^s)$, and the transmitter, $G_t(\varphi^t,\theta^t)$, are both shown in dB. According to this figure, the antennas' radiation patterns do have not isotropic behavior, which consequently leads to different performance to receive/transmit the radio signals in different directions.

Since it supposed that the target has unknown features for the search and localization algorithm (the algorithm doesn't know that the carrier of the transmitter antenna is a ship or a little boat or other sea vehicles.), the measurement model which is used for simulating the real world and the one which is used by the Bayesian filter to estimate the target states are not the same. The first one is a precise model in which the antenna gain, $G_t(\varphi^t,\theta^t)$, is as shown in Fig. 6(b) (in the real world, it is assumed that the transmitter has a helix antenna mounted on a ship depicted in Fig. 6(b)). However, in the second one, the antenna gain is approximated by an Omnidirectional antenna. The difference between the approximated omnidirectional antenna and the real one is considered as the measurement model uncertainty (measurement mismatch modeling).

4- Autonomous search and path planning

The performance of the search and localization algorithm can be enhanced by exploiting appropriate maneuvers or path planning for catching signals that have more information about the target.

4- 1- Autonomous search

The autonomous search approach guides the UAV toward the best detection point (BDP) to catch more efficient signals.

4- 1- 1- Best detection point

The best detection point is a guidance point where the measured signal maximizes the probability of detection. If the event of detection at time step k is denoted by D_k, the probability of detection, given the measurements up to time step k-1, can be computed as

$$P(D_k \mid \mathbf{z}_{k-1}, \mathbf{x}_k^s) = \int P(D_k \mid \mathbf{x}_k^t, \mathbf{x}_k^s) p(\mathbf{x}_k^t \mid \mathbf{z}_{k-1}, \mathbf{x}_{k-1}^s) d\mathbf{x}_k^t \qquad (12)$$

Therefore, the best detection point is

$$x_k^{GP} = \underset{\mathbf{x}_k^s}{\operatorname{argmax}} \, P(D_k \mid \mathbf{z}_{k-1}, \mathbf{x}_k^s) \qquad (13)$$

Using the measurement model described in (11), the detection occurs when the SNR reaches more than a threshold value which is defined as the strength of the received signal when the sensor is located 100 meters far from the target. Therefore, the detection likelihood would be

$$P(D_k \mid \mathbf{x}_k^t, \mathbf{x}_k^s) = \begin{cases} 1 & \|\mathbf{x}^t - \mathbf{x}^s\| \le 100\,m \\ \dfrac{100^2}{\|\mathbf{x}^t - \mathbf{x}^s\|^2} & \|\mathbf{x}^t - \mathbf{x}^s\| > 100\,m \end{cases} \qquad (14)$$

By Monte-Carlo representation of the target posterior, the best detection point can be approximated by Eq. (7).

4- 2- Flying vehicle guidance

To direct the UAV towards the search path, a heuristic guidance law is developed in [30] as follows:

$$\left[\mathbf{a}_g\right]^B = \underbrace{-\mathbf{\eta}\left[\mathbf{v}_k^s\right]^B}_{\text{damping part}} + \underbrace{\mathbf{KR}\left[\mathbf{T}\right]^{BG}\left(\left[x_k^{GP}\right]^G - \left[\mathbf{x}_k^s\right]^G\right)}_{\text{enforcing part}} \qquad (15)$$

This guidance law is comprised of two types of acceleration commands (damping and enforcing parts), which cooperate as a mass-spring-damper system. In Eq. (15), $\left[\mathbf{v}_k^s\right]^B$ is the velocity vector of the UAV, which is expressed in the body coordinate system, $\left[\mathbf{x}_k^s\right]^G$ and $\left[x_k^{GP}\right]^G$ are the position vectors of the UAV and the guidance point, respectively. The guidance point in autonomous search is what is exactly described in Eq. (13), which is expressed in the geographic

coordinate system. Also, $\left[\mathbf{T}\right]^{BG}$ is the transformation matrix from the geographic to the body coordinate system. $\mathbf{ç}$, $\mathbf{K}$, and $\mathbf{R}$ are the damping, conservation, and stochastic matrices, respectively.

The output of this guidance law is, , guidance acceleration command expressed in the UAV body coordinate system, which is applied to the UAV. Ref. [26], developed an acceleration autopilot to translate the guidance acceleration commands to control surfaces of the UAV.

5- Dynamic modeling of UAV

For dynamic modeling of the UAV, the Newton–Euler method is used to derive 6-DOF equations of motion. The translational motion is stated as follows:

$$\frac{d\left[\mathbf{x}^s\right]^G}{dt} = \left[\mathbf{T}\right]^{GB}\left[\mathbf{v}^s\right]^B, \qquad (16)$$

$$m\frac{d\left[\mathbf{v}^s\right]^B}{dt} + m\left[\mathbf{\Omega}^{BG}\right]^B\left[\mathbf{v}^s\right]^B = \left[\mathbf{f}_A + \mathbf{f}_p\right]^B + m\left[\mathbf{T}\right]^{BG}\left[\mathbf{g}\right]^G, \qquad (17)$$

where m is mass, $\mathbf{x}^s$ and $\mathbf{v}^s$ are position and velocity vectors of UAV, respectively, $\mathbf{\dot{U}}^{BG}$ is the skew-symmetric matrix of the angular velocity $\omega^{BG} = \begin{bmatrix} p & q & r \end{bmatrix}^T$, and $\mathbf{f}_A$, $\mathbf{f}_P$, and $\mathbf{g}$ are the aerodynamic and thrust forces and the gravity acceleration, respectively.

The rotational motion is derived as:

$$\begin{bmatrix} \dot{\varphi} \\ \dot{\theta} \\ \dot{\psi} \end{bmatrix} = \begin{bmatrix} 1 & \sin(\varphi)\tan(\theta) & \cos(\varphi)\tan(\theta) \\ 0 & \cos(\varphi) & -\sin(\varphi) \\ 0 & \sin(\varphi)/\cos(\theta) & \cos(\varphi)/\cos(\theta) \end{bmatrix}\left[\mathbf{\omega}^{BG}\right]^B \qquad (18)$$

$$\left[\mathbf{I}^s\right]^B \frac{d\left[\mathbf{\omega}^{BG}\right]^B}{dt} + \left[\mathbf{\Omega}^{BG}\right]^B\left[\mathbf{I}^s\right]^B\left[\mathbf{\omega}^{BG}\right]^B = \left[\mathbf{m}_A\right]^B \qquad (19)$$

where φ, θ, and ψ are roll, pitch, and yaw angles. $\mathbf{I}^s$ is the UAV moment of inertia, and $\mathbf{m}_A$ is the aerodynamic moment that has been exerted on the UAV [37].

6- Simulation results

In this section, several computer simulations have been done to evaluate the performance of the proposed method.

6- 1- Simulation outline

In the simulation outline, an "Aerosonde" unmanned fixed-wing aircraft attempts to search for a lost target within 40 km by 40 km marine area. The UAV starts from its home position [-35, 35, -0.2]^T km and moves with constant speed and at height h=200 m. The coordinate system is local NED (North-East-Down) in which the z-direction is toward the earth down, and its origin is a point on the earth's surface.

Table 1. Simulation parameters.

Parameter	Value
UAV velocity	30 m/s
Target velocity	5 m/s
Transmitter antenna power	10 Watt
SNR	[10 - 20] dB
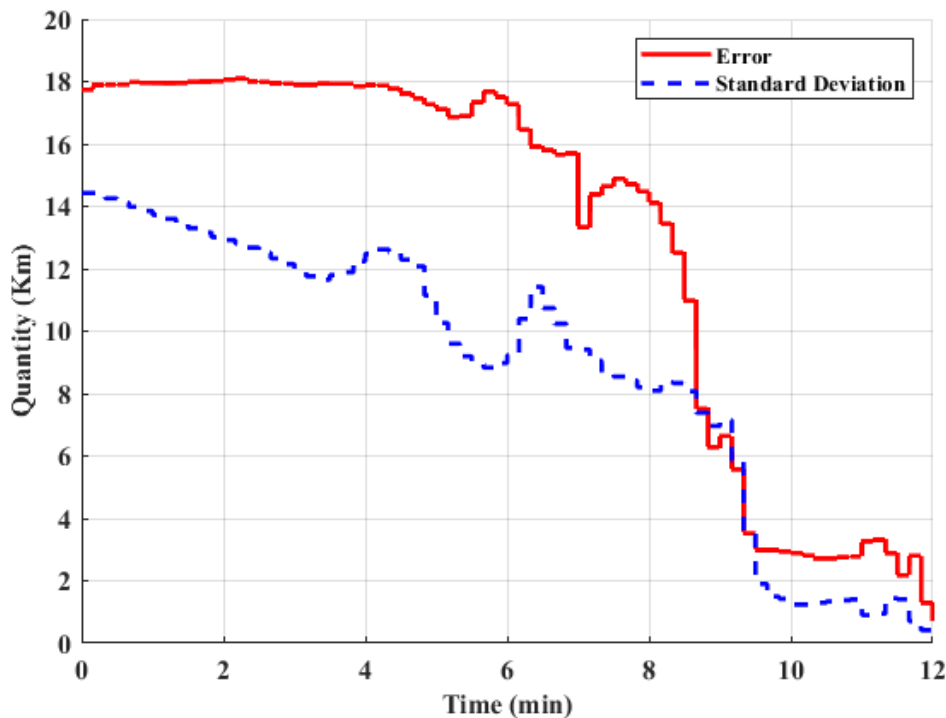
Fig. 7. The trend of position error and posterior standard deviation in one of the simulations.

The search and localizing algorithm will be terminated when the standard deviation of the posterior reaches less than a specified value. This moment is called the detection time, and the actual distance between the target and the estimated positions is the estimation error. The transmitter antenna power is set to 10 watts to provide strong received signal strength (>−80 dBm) to ensure reliable connection and suppress ambient RF interference [38]. Since it is assumed that there is no accurate information about the target, the uncertainty of the receiver antenna power is modeled by a Gaussian distribution with a mean of 0.5 watts. Simulation parameters are reported in Table 1.

6- 2- Monte-Carlo simulations

To statistically evaluate the performance of the proposed localization algorithm, 100 simulations are performed. In every run, the target is uniformly located over the search area with different heading directions (because the target heading affects the received signal strength by the UAV).

Fig. 7 represents the trend of position error as well as the posterior standard deviation of position for one sample of the simulations. The descending trend of both quantities indicates that if the standard deviation becomes below a threshold, the target position has been estimated sufficiently close to the actual target location (since the UAV doesn't know the actual

Table 2.Comparison of two, with and without measurement model mismatch scenarios.

		Localization error (m)	
Assumption	Success (%)	Mean	RMSE[1]
Accurate model	97	9.51	742
Uncertain model	88	8.93	838
Model Ref. [30]	--	5.97	4065

[1]Root Mean Square Error

estimation error, it should employ the standard deviation of the target posterior for terminating the localization algorithm).

Accordingly, a search is terminated when the posterior standard deviation of the target position becomes below 200 meters. Then a search mission is called successful if the position error between the real target position and the estimated one reaches below 1 kilometer within 30 minutes.

6- 3- Results

As previously mentioned, it is desired that the developed algorithm be robust against the measurement model mismatches. Therefore, in Table 2, the performances of three scenarios with three different assumptions for the type of transmitter antenna are compared.

- Scenario 1 (Helix): Complete information on the transmitter antenna is available. So, there are no mismatches between the real world (simulations) and the measurement model used by the Bayesian filter. In other words, the helix antenna gain shown in Fig. 5(b) that is considered for real-world simulations is also as transmitter antenna gain in Eq. (10) (Bayesian filter measurement model).
- Scenario 2 (Omni-Directional): It is assumed that there is no information about the type of transmitter antenna. Therefore, same as scenario 1, the helix antenna gain shown in Fig. 5(b) is used for the real world but it is assumed that the transmitter antenna gain pattern (employed by the Bayesian filter (Eq. (10))) is omnidirectional. So, there is mismatch between the real world (simulations) and

the measurement model. The radiation pattern for an omnidirectional antenna is uniform in horizontal directions and varies in different elevation angles.
- Scenario 3 (Spherical): Ref. [30] assumed that the radiation pattern of receiver and transmitter antennas are isotropic in all directions. In this scenario, there is a further mismatch between the simulation and the measurement model.

For a more intuitive understanding of the evaluation criteria mentioned in Table 2, the results are also represented in Fig. 8. The search approach, utilizes the searching guidance law (Eq. 15) to perform more appropriate maneuvers to capture more efficient signals, which results in high success rate in low SNR environments. The small difference between the results of scenarios 1 (Helix assumption, perfect measurement model) and 2 (Omni-Directional assumption) indicates that the developed algorithm is robust to the uncertainties of the measurement model. The high localization error of scenario 3 indicates that the spherical assumption of the antenna radiation pattern is not correct. Therefore, the best assumption for modeling the mismatch between the actual transmitter antenna and the approximated one is omnidirectional.

Fig. 9-11 depicts the trend of target state estimates in three samples of Monte-Carlo simulations. The UAV motion increases the observability of the target position and its estimate converges to real one. In these figures, black, blue, and red empty circles represent the initial target position, initial estimate of target position, and initial UAV position, respectively. Black, blue, and red solid squares are also the final position of the target, the final estimate of the target
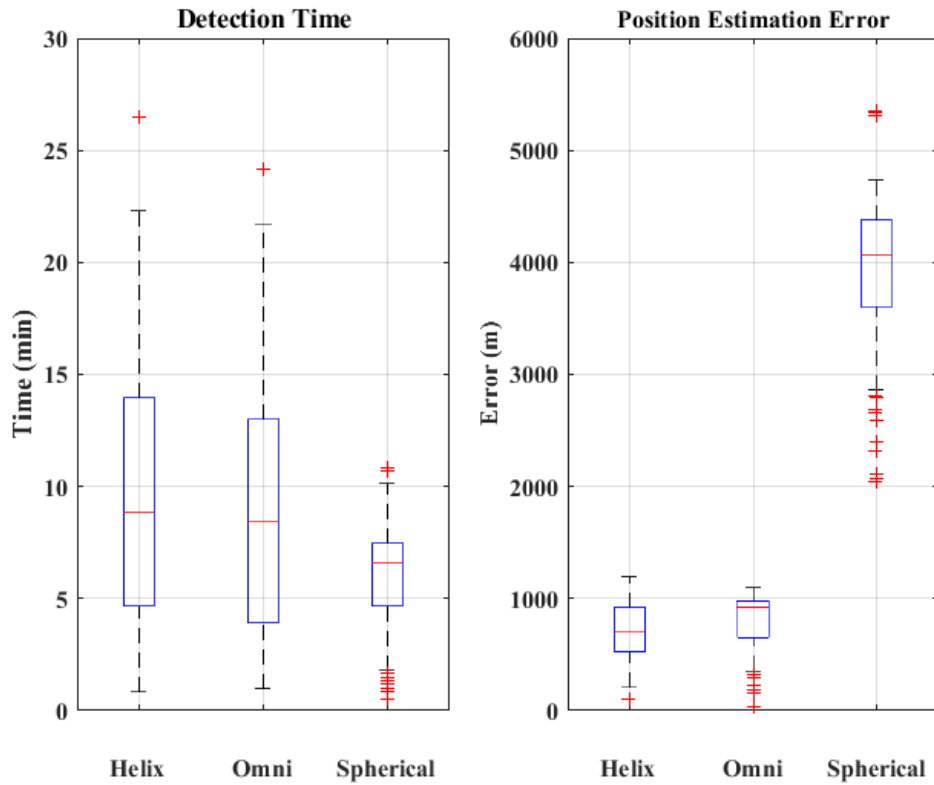
Fig. 8 .Box plot comparison of three scenarios.

position, and the final position of the UAV, respectively. Black and red solid lines are the trajectory of the target and the UAV, respectively. In addition, the blue dots are the trend of target position estimates. In all of these samples, it is shown that the algorithm can track the moving target before target detection.

To understand more about the statistical trend of SMC samples and their corresponding weight distribution, which is explained in section 2, six-time snapshots of simulation depicted in Fig. 9 are illustrated in Fig. 12. The weight assigned to each particle has been specified by the rainbow scale. Since the chance of target presence is equal for any part of the search area, the initial probability distribution of the target position is modeled by a uniform distribution. Hence, according to the nonlinear localizing problem, the non-Gaussian prior leads to a non-Gaussian posterior, sequentially. Contrary to the Kalman filter, the SMC filter can estimate the non-Gaussian posterior distribution of target position states as well as shown by the snapshots.

7- Conclusion

The present research proposed a Track-Before-Detect approach to search and localize a lost target in a wide marine environment using only RSS measurement by an antenna mounted on a UAV. Both the transmitter and receiver antennas were designed and customized with an accurate radiation pattern model for a search and rescue scenario in a wide marine environment.

The SMC implementation of the Bayesian filter provides a suitable framework for dealing with problem challenges, including nonlinear models, non-Gaussian prior and noises, target unknown dynamics, and uncertainty of target properties.

The proposed search approach applies more appropriate maneuvers to the UAV to capture more efficient signals, utilizing a heuristic searching guidance law and guidance points, which result in less localization error in low SNR environments.

To evaluate the performance of the proposed method, three scenarios have been performed with three different assumptions for the type of transmitter antenna. The radiation pattern of the transmitter antenna, in the scenario that there is measurement model uncertainty, was approximated by an omnidirectional antenna. Comparative evaluation of scenarios 1 (Helix assumption, perfect measurement model) and 2 (Omni-Directional assumption) indicates the robustness of the filter against the target uncertainties. Meanwhile, scenario 3 (spherical assumption of the antenna radiation pattern) leads to high localization error. Therefore, the best assumption for modeling the mismatch between the actual transmitter antenna and the approximated one is omnidirectional.

Data availability

Some or all data, models, or codes that support the findings of this study are available from the corresponding author upon reasonable request.
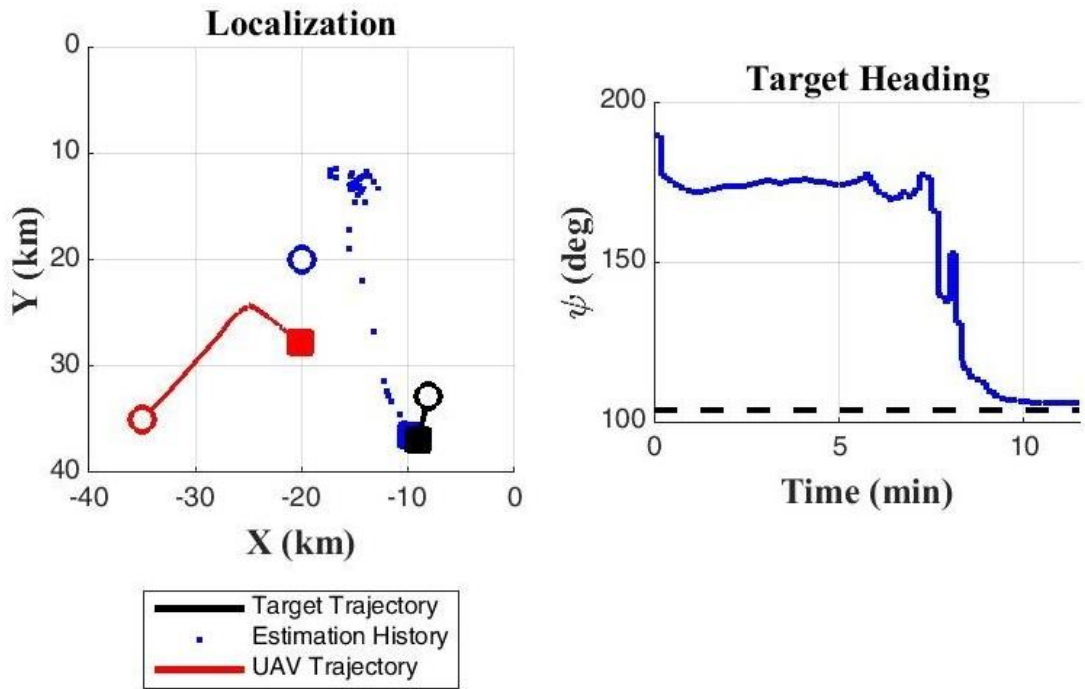
Fig. 9 . Monte-Carlo simulations: sample 1. start/end position has shown b ●/■.   .
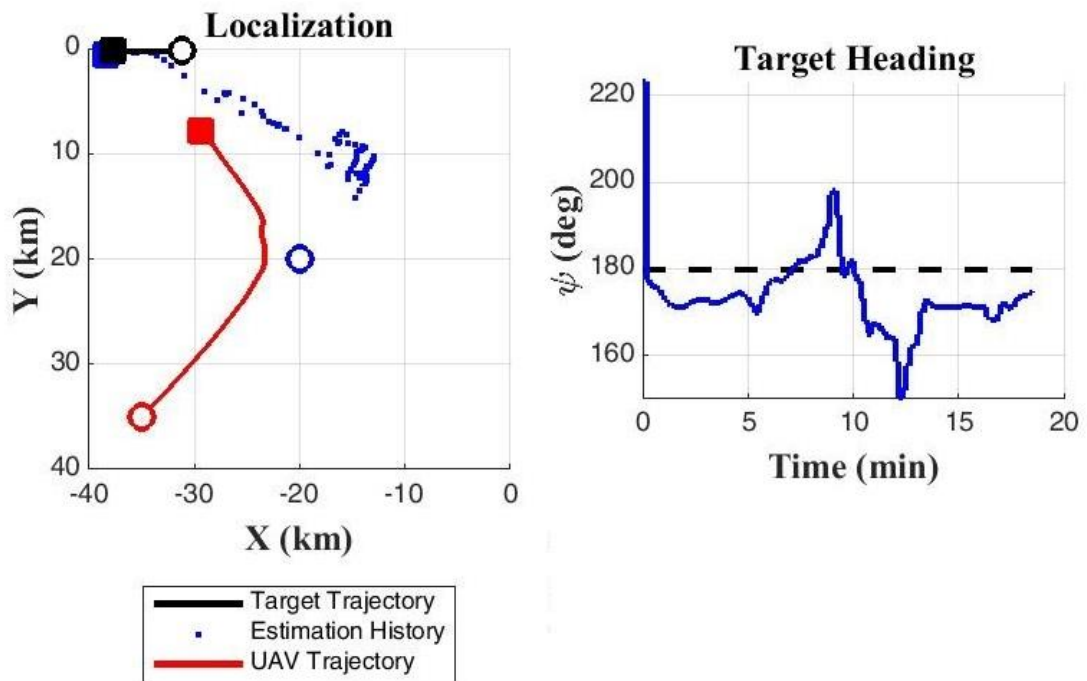
Fig. 10. Monte-Carlo simulations: sample 2. start/end position has shown by ●/■.   .
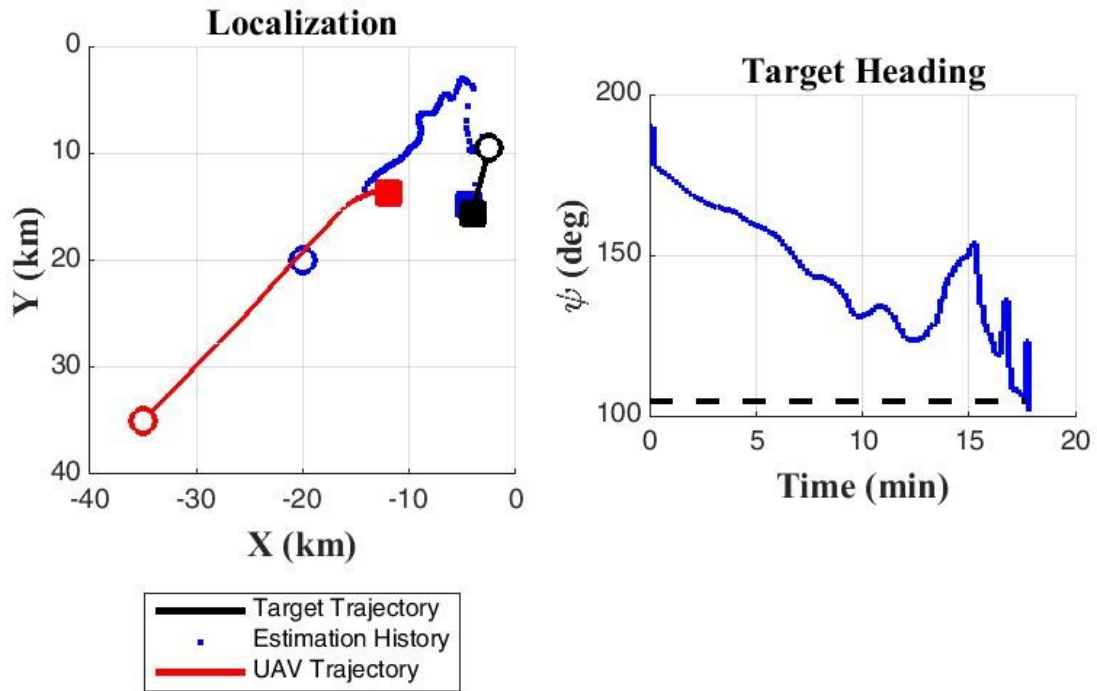
Fig. 11. Monte-Carlo simulations: sample 3. start/end position has shown by ○/■.
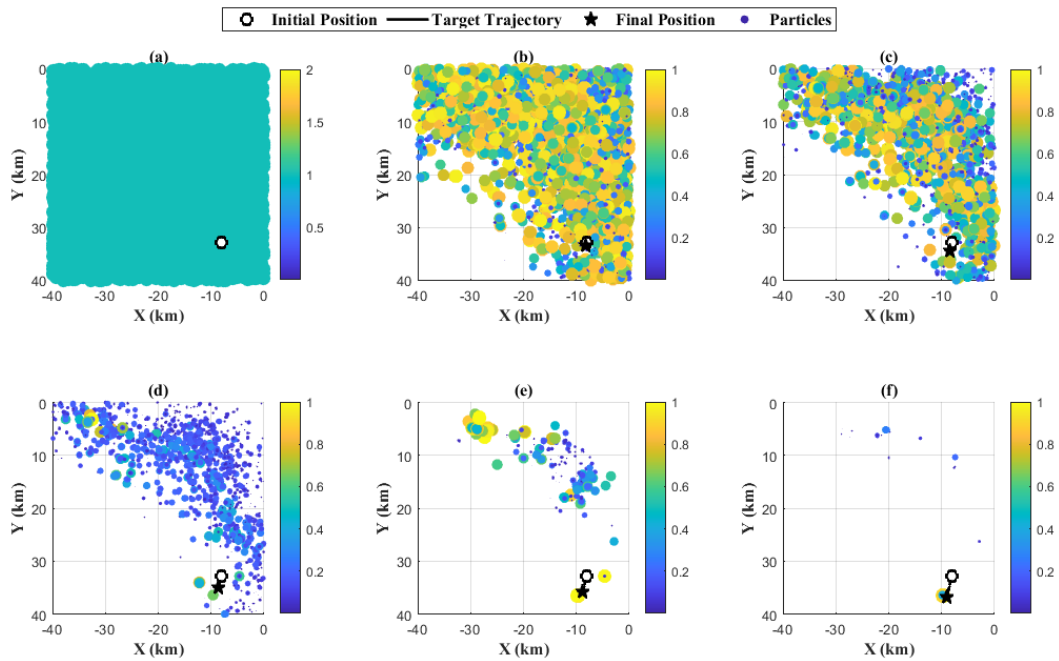
Fig. 12. Six time snapshots of the second simulation. (a) Time=0 min. (b) Time=2 min. (c) Time=4 min. (d) Time=6 min. (e) Time=8 min. (f) Time=11 min.

Nomenclature

$\mathbf{x}^t$	=	state vector of target	$\mathbf{x}^s$	=	state vector of seeker
x^t	=	target position (x-axis)	y^t	=	target position (y-axis)
$\mathbf{w}_k$	=	dynamic noise vector	$\mathbf{v}_k$	=	measurement noise vector
$\mathbf{z}_{1:k}$	=	measurement history	ψ^t	=	target heading
P_s	=	received antenna power	G_s	=	receiver antenna gain
P_t	=	transmitter antenna power	G_t	=	transmitter antenna gain
λ	=	signal wavelength	a	=	acceleration command
ω	=	angular velocity			

Superscripts

t	=	target	S	=	seeker
B	=	body coordinate system	G	=	geographic coordinate system

Subscripts

k	=	time step
A	=	aerodynamic
g	=	guidance

References

[1] A. Milan, S. H. Rezatofighi, A. R. Dick, I. D. Reid, and K. Schindler, "Online Multi-Target Tracking Using Recurrent Neural Networks.," in AAAI, 2017, p. 4.

[2] L. G. Santesteban, S. F. Di Gennaro, A. Herrero-Langreo, C. Miranda, J. B. Royo, and A. Matese, "High-resolution UAV-based thermal imaging to estimate the instantaneous and seasonal variability of plant water status within a vineyard," Agric. Water Manag., vol. 183, pp. 49–59, 2017.

[3] O. M. Cliff, R. Fitch, S. Sukkarieh, D. Saunders, and R. Heinsohn, "Online Localization of Radio-Tagged Wildlife with an Autonomous Aerial Robot System.," in Robotics: Science and Systems, 2015.

[4] S. Manickam, S. C. Swar, D. W. Casbeer, and S. G. Manyam, "Multi-unmanned aerial vehicle multi acoustic source localization," Proc. Inst. Mech. Eng. Part G J. Aerosp. Eng., vol. 235, no. 3, pp. 273–294, Mar. 2021, doi: 10.1177/0954410020943086.

[5] N. A. Khan, N. Z. Jhanjhi, S. N. Brohi, R. S. A. Usmani, and A. Nayyar, "Smart traffic monitoring system using unmanned aerial vehicles (UAVs)," Comput. Commun., vol. 157, pp. 434–443, 2020.

[6] B. Bayat, N. Crasta, A. Crespi, A. M. Pascoal, and A. Ijspeert, "Environmental monitoring using autonomous vehicles: a survey of recent searching techniques," Curr. Opin. Biotechnol., vol. 45, pp. 76–84, 2017.

[7] L. F. Gonzalez, G. A. Montes, E. Puig, S. Johnson, K. Mengersen, and K. J. Gaston, "Unmanned aerial vehicles (UAVs) and artificial intelligence revolutionizing wildlife monitoring and conservation," Sensors, vol. 16, no. 1, p. 97, 2016.

[8] J. C. Hodgson, S. M. Baylis, R. Mott, A. Herrod, and R. H. Clarke, "Precision wildlife monitoring using unmanned aerial vehicles," Sci. Rep., vol. 6, no. 1, pp. 1–7, 2016.

[9] Y. Liu, Z. Liu, J. Shi, G. Wu, and C. Chen, "Optimization of base location and patrol routes for unmanned aerial vehicles in border intelligence, surveillance, and reconnaissance," J. Adv. Transp., vol. 2019, 2019.

[10] Y. Kang, Q. Wang, J. Wang, and R. Chen, "A high-accuracy TOA-based localization method without time synchronization in a three-dimensional space," IEEE Trans. Ind. Inform., vol. 15, no. 1, pp. 173–182, 2018.

[11] P. Wan, Q. Huang, G. Lu, J. Wang, Q. Yan, and Y. Chen, "Passive localization of signal source based on UAVs in complex environment," China Commun., vol. 17, no. 2, pp. 107–116, 2020.

[12] X. Liu et al., "Kalman filter-based data fusion of wi-fi rtt and pdr for indoor localization," IEEE Sens. J., vol. 21, no. 6, pp. 8479–8490, 2021.

[13] Y. Wang and K. C. Ho, "An asymptotically efficient estimator in closed-form for 3-D AOA localization using a sensor network," IEEE Trans. Wirel. Commun., vol. 14, no. 12, pp. 6524–6535, 2015.

[14] R. M. Vaghefi, M. R. Gholami, R. M. Buehrer, and E. G. Strom, "Cooperative received signal strength-based sensor localization with unknown transmit powers," IEEE Trans. Signal Process., vol. 61, no. 6, pp. 1389–1403, 2012.

[15] S. Tomic, M. Beko, and R. Dinis, "RSS-based localization in wireless sensor networks using convex relaxation: Noncooperative and cooperative schemes," IEEE Trans. Veh. Technol., vol. 64, no. 5, pp. 2037–2050, 2014.

[16] B. Yang, L. Guo, R. Guo, M. Zhao, and T. Zhao, "A novel trilateration algorithm for RSSI-based indoor localization," IEEE Sens. J., vol. 20, no. 14, pp. 8164–8172, 2020.

[17] Z. Wang, H. Zhang, T. Lu, and T. A. Gulliver, "Cooperative RSS-based localization in wireless sensor networks using relative error estimation and semidefinite programming," IEEE Trans. Veh. Technol., vol. 68, no. 1, pp. 483–497, 2018.

[18] P. Zuo, T. Peng, K. You, W. Guo, and W. Wang, "RSS-based localization of multiple directional sources with unknown transmit powers and orientations," IEEE Access, vol. 7, pp. 88756–88767, 2019.

[19] H. Kwon and I. Guvenc, "RF Signal Source Search and Localization Using an Autonomous UAV with Predefined Waypoints," ArXiv Prepr. ArXiv230107027, 2023.

[20] S. A. A. Shahidian and H. Soltanizadeh, "Optimal path planning for two unmanned aerial vehicles in DRSS localization," Int. J. Control Autom. Syst., vol. 16, no. 6, pp. 2906–2914, 2018.

[21] X. Shi, Y. H. Chew, C. Yuen, and Z. Yang, "A RSS-EKF localization method using HMM-based LOS/NLOS channel identification," in 2014 IEEE International Conference on Communications (ICC), IEEE, 2014, pp. 160–165.

[22] F. Koohifar, A. Kumbhar, and I. Guvenc, "Receding horizon multi-UAV cooperative tracking of moving RF source," IEEE Commun. Lett., vol. 21, no. 6, pp. 1433–1436, 2016.

[23] S. A. A. Shahidian and H. Soltanizadeh, "Path planning for two unmanned aerial vehicles in passive localization of radio sources," Aerosp. Sci. Technol., vol. 58, pp. 189–196, 2016.

[24] Y. Liu, J. Zhou, L. Wang, Y. Wang, Y. Yin, and Z. Ding, "Radio Frequency Identification target location based on the Unmanned Aerial Vehicle," in Journal of Physics: Conference Series, IOP Publishing, 2022, p. 012085.

[25] M. Jouin, R. Gouriveau, D. Hissel, M.-C. Péra, and N. Zerhouni, "Particle filter-based prognostics: Review, discussion and perspectives," Mech. Syst. Signal Process., vol. 72, pp. 2–31, 2016.

[26] N. Wagle and E. Frew, "A particle filter approach to wifi target localization," in AIAA guidance, navigation, and control conference, 2010, p. 7750.

[27] H. Van Nguyen, M. Chesser, L. P. Koh, S. H. Rezatofighi, and D. C. Ranasinghe, "Trackerbots: Autonomous uav for real-time localization and tracking of multiple radio-tagged animals," ArXiv Prepr. ArXiv171201491, vol. 33, 2017.

[28] S. M. Esmailifar and F. Saghafi, "Cooperative localization of marine targets by UAVs," Mech. Syst. Signal Process., vol. 87, pp. 23–42, 2017.

[29] S. M. Esmailifar and F. Saghafi, "Moving target localization by cooperation of multiple flying vehicles," IEEE Trans. Aerosp. Electron. Syst., vol. 51, no. 1, pp. 739–746, 2015.

[30] F. Saghafi and S. M. Esmailifar, "Searching and localizing a radio target by an unmanned flying vehicle using bootstrap filtering," J. Dyn. Syst. Meas. Control, vol. 137, no. 2, p. 021008, 2015.

[31] D. Simon, Optimal state estimation: Kalman, H infinity, and nonlinear approaches. John Wiley & Sons, 2006.

[32] N. J. Gordon, D. J. Salmond, and A. F. Smith, "Novel approach to nonlinear/non-Gaussian Bayesian state estimation," in IEE Proceedings F-radar and signal processing, IET, 1993, pp. 107–113.

[33] N. Bergman, "Recursive bayesian estimation," Dep. Electr. Eng. Linköping Univ. Linköping Stud. Sci. Technol. Dr. Diss., vol. 579, p. 11, 1999.

[34] B. Ristic, S. Arulampalam, and N. Gordon, Beyond the Kalman filter: Particle filters for tracking applications. Artech house, 2003.

[35] H. T. Friis, "A note on a simple transmission formula," Proc. IRE, vol. 34, no. 5, pp. 254–256, 1946.

[36] S. Šain, "Modelling and characterization of wireless channels in harsh environments," PhD Thesis, Master's thesis, Mälardalen University, 2011.

[37] P. H. Zipfel, "Modeling and Simulation of Aerospace Vehicle Dynamics (Aiaa Education)," AIAA Am. Inst. Aeronaut. Ast, 2003.

[38] B. Yamamoto et al., "Received signal strength indication (RSSI) of 2.4 GHz and 5 GHz wireless local area network systems projected over land and sea for near-shore maritime robot operations," J. Mar. Sci. Eng., vol. 7, no. 9, p. 290, 2019.